Supplementary Materials for

In vivo Perturb-Seq reveals neuronal and glial abnormalities associated with autism risk genes

Xin Jin[1,2,3,4,*], Sean K. Simmons[3,5,6], Amy Guo[3], Ashwin S. Shetty[2], Michelle Ko[2], Lan Nguyen[3,6], Vahbiz Jokhi[2], Elise Robinson[3,5,8], Paul Oyler[2], Nathan Curry[2], Giulio Deangeli[2], Simona Lodato[7], Joshua Z. Levin[3,5,6], Aviv Regev[3,6,9,10,*,†], Feng Zhang[3,4,10,*,†], and Paola Arlotta[2,3,5,*,†]

Correspondence to: Xin Jin (xinjin@fas.harvard.edu), Aviv Regev (aregev@broadinstitute.org), Feng Zhang (zhang@broadinstitute.org), and Paola Arlotta (paola_arlotta@harvard.edu).

This PDF file includes:

Materials and Methods

Lentiviral vector construction and production

Lentiviral vectors were constructed as previously reported (*11-13*). The backbone plasmid contains antiparallel cassettes of two gRNAs (**Table S5**) under mouse U6 and human U6 promoters, and the EF1a promoter to express puromycin, BFP, and a polyadenylated barcode unique to each perturbation. Cloning of the 38 vectors were done individually. Association of each gRNA set and perturbation barcode was established by Sanger sequencing. The gRNA designs were defined using the online tool at benchling.com (*49*). Each lentivirus was packaged individually with the V2 helper plasmids (*50*), and the functional titer was measured individually through HEK293 cell infection and FACS measurement of the BFP^+ population before pooling equally for ultracentrifugation. The functional titer of the final lentivirus was > 5 x 10^9 U/mL for *in utero* ventricular injection and transduction.

In vivo Perturb-Seq experiment

All animal experiments were performed according to protocols approved by the Institutional Animal Care and Use Committees (IACUC) of Harvard University and of the Broad Institute of MIT and Harvard.

This analysis comprises 17 independent libraries of Perturb-Seq cells. *In utero* lentiviral injection into the lateral ventricles was performed at E12.5 in Cas9 transgenic mice (*14*) (4-6 month old, Jax#026179), and each 10x single-cell library was made by combining the BFP^+ cells from 1-3 litters (4-20 animals) of P7 animals harvested on the same day.

P7 mice were anesthetized then disinfected with 70% ethanol and decapitated. The brains were quickly extracted into ice-cold PBS and cortices were micro-dissected in ice-cold Hibernate A medium (BrainBits, #HA-Lf) with B27 supplement (ThermoFisher, #17504044) under a dissecting microscope. Tissue dissociation was performed with the Papain Dissociation kit (Worthington, #LK003152) in a modification of a previously described protocol (*51*).. Briefly, cortices were transferred into ice-cold papain solution with DNase in a cell culture dish and cut into small pieces with a blade. The dish was then placed onto a digital rocker in a cell culture incubator for 30 mins with rocking speed at 30 rpm at 37°C. The digested tissues were collected into a 15 mL tube with 5 mL of EBSS buffer (from the Worthington kit). The mixture was triturated with a 10 mL plastic pipette 20 times and the cell suspension was carefully transferred to a new 15 mL tube. 2.7 mL of EBSS, 3 mL of reconstituted Worthington inhibitor solution, and DNAse solution were added to the 15 mL tube and mixed gently. Cells were pelleted by centrifugation at 300 g for 5 mins at RT. Cells were resuspended in 0.5 mL ice-cold Hibernate A with B27 supplement (ThermoFisher, A3582801) and 10% fetal bovine serum (FBS) and subjected to FACS purification. The FACS collected cells were sorted

in cold Hibernate A/B27 medium with 10% FBS (VWR, #97068). After collection, the cells were centrifuged and resuspended in ice-cold PBS with 0.04% BSA (NEB, B9000S) for single-cell RNA sequencing library preparation (10x Genomics v2 chemistry). We performed the FACS purification and resuspension within 1.5 h while keeping the cells on ice to prevent necrosis.

RNA *in situ* hybridization

Multiplexed RNAscope fluorescent *in situ* hybridization was performed on fixed-frozen tissue. Mice were anesthetized and transcardially perfused with ice-cold PBS followed by ice-cold 4% paraformaldehyde in PBS. Dissected brains were postfixed overnight in 4% paraformaldehyde at 4°C, and cryoprotected in 30% sucrose. Brains were then embedded in optimal cutting temperature (OCT) compound (Tissue-Tek, #4583) and 15-20μm tissue sections were prepared.

Multiplex RNAscope v1 was performed based on manufacturer's instructions. Probes against the following mRNA were used: *Pdgfra*, *Cspg4*, and *Fezf2* (ACDBio). We double-blinded the staining, imaging, and quantifications. Quantification was performed using the StarSearch program (https://www.seas.upenn.edu/~rajlab/StarSearch/launch.html).

Immunohistochemistry

Mice were anesthetized and transcardially perfused with ice-cold PBS followed by ice-cold 4% paraformaldehyde in PBS. Dissected brains were postfixed overnight in 4% paraformaldehyde at 4 °C, and cryoprotected in 30% sucrose. The brains were embedded in OCT compound (Tissue-Tek, #4583) and 15μm tissue sections were prepared. The slides with tissue sections were incubated with blocking media (6% donkey serum in 0.3% Triton with PBS) for 1hr, then incubated with primary antibodies in the incubation media (1:3 dilution of blocking media in PBS with 0.3% Triton) overnight at 4 °C. Slides were washed with PBS with 0.3% Triton 4 times to remove the excess primary antibody. Secondary antibodies were applied at 1:800 dilution in blocking media and incubated for 2hr at room temperature. Slides were then washed 4 times with PBS with 0.3% Triton, and incubated with DAPI for 10 mins before mounting with Fluoromount G (Invitrogen, #00-4958-02). The antibodies and dilutions were: Mouse anti-NeuN antibody (mab377, 1:500; Millipore), Mouse anti-GS antibody (mab302, 1:500; Millipore), Goat anti-Pdgfra antibody (AF1062, 1:200; R&D System), Rabbit Iba1 antibody (019-19741, 1:400; Wako), Chicken anti-GFP antibody (ab16901, 1:500; Millipore), Mouse anti-Satb2 (ab51502, 1:50; Abcam), Rat anti-Ctip2 (ab18465, 1:100, Abcam), Rabbit anti-Sox6 (ab30455, 1:500; Abcam), Rat anti-Mbp (mab386, 1:100; Millipore).

All images were acquired using either a custom-built spinning disk confocal microscope equipped with image acquisition NIS-Elements software, or a Carl Zeiss epifluorescent microscope with Zen software. To quantify protein expression levels, we divided the

thickness of the cortex into bins, and calculated the average pixel value per bin. For this, we double-blinded the staining, imaging, and quantifications.

Perturb-Seq profiling

Single-cell RNA sequencing libraries were created using the Chromium Single Cell 3' Solution v2 kit (10x Genomics) following the manufacturer's protocol. Each library was sequenced with Illumina NextSeq high-output 75-cycle kit with sequencing saturation above 70%. Reads were aligned to the mm10 mouse genome reference using the Cell Ranger package (10x Genomics).

To sequence the perturbation barcode, dial-out PCR was performed to extract the perturbation barcode in each cell. This is modified from Dixit et al (*12*) to be compatible with the 10x Genomic V2 chemistry instead of V1. The PCR product was sequenced along with the 10x libraries, and demultiplexed to extract the perturbation information.

Forward primer:
CAAGCAGAAGACGGCATACGAGAT-TCGCCTTA-
GTCTCGTGGGCTCGGAGATGTGTATAAGAGACAG-
TAGCAAACTGGGGCACAAGC
Reverse primer (i5):
AATGATACGGCGACCACCGAGATCTACAC

Data pre-processing

BCL files were transformed into fastq files using the cellranger mkfastq command, using CellRanger V2.1.0. Bam files and expression matrices were generated from these fastq files using the cellranger count command, using force_cells=8000.

Identification of perturbation barcode

We identified perturbation barcodes by two complementary methods. To extract perturbation information from the dial-out reads, we modified code from the original Perturb-Seq work (*12*) to work with 10x V2 chemistry, and applied it to our data (original code at https://github.com/asncd/MIMOSCA). This resulted in a cell-by-perturbation UMI count matrix. To extract perturbation information from the 10x reads, a fasta file was first created with one entry for each perturbation, containing the sequence of the perturbation barcode and the surrounding sequence. This fasta file was turned into a STAR reference (*52*), referred to as the PBC reference. Unmapped reads containing either AGAATT or CCTAGA as a subsequence were extracted from the Cell Ranger bam file, and then mapped to this new reference. Low quality reads were filtered out using the following filters: (i) used "samtools view -F 2820" to filter out unmapped, multimapped, and low quality reads from the PBC mapped bam file, (ii) removed reads with quality

scores <255, (iii) removed reads whose 5' end did not map between 655 and 714bp into the PBC reference, to help exclude reads that did not overlap enough bases in the perturbation barcode for proper identification of the perturbation, and (iv) removed reads whose edit distance from the PBC reference was >2. Reads were then assigned to the perturbation they mapped best. Cell barcodes and UMIs were extracted, and a cell-by-perturbation UMI count matrix was created. This matrix was used to assign cells to perturbations in the same way as with the dial-out data. As with the dialout data, if a cell had one perturbation with >1.3x the number of UMIs assigned to it than the next best perturbation based on the 10x sequence, that cell was assigned to that perturbation in the 10x data; otherwise, the cell was declared to have multiple perturbations. We then only kept cells for which either i) the assigned 10x and dialout perturbations agree or ii) the cell was assigned to a perturbation by one method but not assigned to any perturbation in the other.

Cell type clustering analysis

UMI count data was loaded into R and processed using the Seurat v 2.2 package (*48*). Data were scaled to counts per million and log normalized. Cells expressing less than 500 genes were removed. Variable genes were found using FindVariableGenes with x.low.cutoff=1 for each batch separately. Genes that were found to be variable in at least 4 batches were combined into a final combined list of variable genes. The normalized data was scaled with ScaleData on the variable genes, regressing out the effects of nUMI, and PCA was performed. Clustering was performed with the FindClusters function (with default parameters, except for resolution=1.2 and using 28 PCs). tSNE plots were generated with RunTSNE (RunTSNE (with default parameters, except with 17 PCs and pca=F). Clusters were assigned to cell types based on marker genes from the literature, mousebrain.org (*16*), and DropViz (*23*). For each cell type a more refined nGene cutoff was identified (**fig. S3**), and cells of that cell type with less than that filter were removed from further consideration. Cell clustering does not follow the proportion of mitochondrial reads or nUMI in each cell. We focused only on cells of 5 key types (projection neurons, inhibitory neurons, oligodendrocytes, microglia/macrophages, and astroglia) and removed the rest.

For subclustering individual cell types, the cells of that cell type were extracted from the larger Seurat object. Variable genes were chosen as above, and data was scaled with ScaleData, regressing out the effects of nUMI and batch, followed by PCA. Clustering was performed with FindClusters (with default parameters except for varying resolutions and number of PCs, **Table S6**). tSNE was performed with RunTSNE (with default parameters, except with different numbers of PCs and pca=F).

Testing WGCNA gene sets

WGCNA was performed for each cell cluster based on the published pipeline (*22*). We manually removed modules that were driven by outlier cells (these are modules that are highly expressed in a very small number of cells; this is the module level quality control, equivalent of filtering out genes expressed in a small number of cells). For a given cell type, each WGCNA gene set was input into moduleEigengenes to calculate a gene-set score for that set of genes. All cells without an assigned perturbation were removed.

Linear regression was used to test the relationship between perturbations and WGCNA gene scores, correcting for batch and number of genes with the lm function in R, using the formula:

Gene Score ~ perturbation + batch + nGene

Associated *P-values* and effect sizes were extracted. In addition, a permutation-based approach was used to calculate an empirical *P-value* to ensure the model-based *P-values* reported by lm were accurate. Specifically, the perturbation labels of cells were randomly permuted within each batch, and the absolute effect size for each perturbation was calculated as above on this permuted data. This was repeated 10,000 times. The empirical *P-value* was the proportion of permutations (including the original data) with absolute effect size larger than that of the original data. FDR correction was performed using the Benjamini & Hochberg procedure.

To implement alternative analytical assumptions that do not rely on individual cells being independent conditional on batch, we took a linear mixed model-based approach. We used the lmer function from the lmerTest package in R. For each module, we used this function to fit a linear mixed model of the scaled module scores with random interaction effect for each batch/perturbation pair, and fixed effects for batch, perturbation, and scaled nGene. This was performed with the R formula:

WGCNA_Score ~ batch + perturbation + nGene + (1|batch:perturbation)

where WGCNA_Score and nGene were mean centered and normalized to have variance 1. The p-values and effect sizes for each perturbation were then extracted from the resulting model.

Structural Topic Modelling

Structural topic modelling (STM) was performed separately on each cell type of interest using the STM package in R (*21*). Count data from cells of a given type were extracted from the Seurat object, along with corresponding meta data. Genes that occurred in <5% or >90% of cells were removed, as were mitochondrial and ribosomal genes. In addition,

only genes that were expressed in at least one cell in all batches were retained in order to help reduce batch effects. The resulting count matrix was provided as input to the STM function, along with the meta data and with parameters LDAbeta=T, interactions=F. The formula used by the STM function was

~ perturbation + batch + nGene

This specifies a model that assumed topic proportions were dependent on perturbation, number of genes, and batch. We ran this model on each dataset with 5 topics. Top 10 genes for each topic were extracted with the labelTopics function.

To test for correlations between perturbations and topics, the theta matrix (the matrix containing proportions of topics per cell) was extracted from the STM matrix. For each topic, linear regression was used to test how the per-cell proportions for each topic related to perturbations (after setting GFP to be the reference perturbation), correcting for nGene and batch. In particular, the lm function in R was used, with the formula:

Proportion Topic ~ perturbation + batch + nGene

Effect sizes were extracted from the resulting lm object. An empirical *P-value* was calculated, as for WGCNA. FDR correction was performed using the Benjamini & Hochberg procedure.

Correlation graph of WGCNA genes

For each cell type, all genes that appeared in at least one module for that cell type were extracted and the correlation between each pair was calculated. An 11 nearest neighbor graph was constructed, and the results were plotted with the igraph (v1.2.4.1) plot feature.

Analysis of human single nucleus or single cell RNA-seq data

For each single cell/nucleus human dataset, the UMI count matrix and meta data were downloaded (adult human data (*30*): https://portal.brain-map.org/atlases-and-data/rnaseq/human-multiple-cortical-areas-smart-seq/, fetal human data (*32*): https://cortex-dev.cells.ucsc.edu/, human cerebral organoids data (*33*): https://singlecell.broadinstitute.org/single_cell/study/SCP282/reproducible-brain-organoids/) and processed with Seurat to create Seurat objects, with no nGene cutoff. Cell types were extracted from the metadata, and combined into more general cell types, namely: Microglia, Astroglia (including Radial Glia), Inhibitory neurons, and Excitatory neurons, ODCs, and others. Correlation analysis was then performed on these data as described in the ‘Correlation Analysis’ section.

Gene module conservation and modularity: Correlation Analysis

For each dataset and each module, the associated cell type was extracted. The number of genes in the module expressed in at least 1% or 5% of cells were calculated. All genes expressed in <5% of cells were then excluded, as were modules with <3 genes surviving this 5% cutoff. The Pearson correlation coefficient between each pair of genes in the module was calculated, and the mean of these coefficients was calculated. For each module, a null distribution of the mean correlation coefficient was calculated as follows: a random set of genes was chosen with the same number of genes as the WGCNA module and roughly the same expression levels (all genes expressed by that cell type were partitioned into 100 mean expression bins, and randomly sampled genes from the matched bin for each gene in the module), and the average correlation coefficient was calculated as above. This was repeated 1,000 times, and an empirical *P-value* was estimated as the proportion of gene sets with correlation greater than that in the WGCNA module, as was an expected value for this average correlation coefficient. The normalized correlation was calculated by dividing the average correlation of the WGCNA module by the standard deviation of the correlation value from the matching null distribution and subtracting the mean correlation. Confidence intervals were calculated using bootstrapping (boot package v1.3-20 in R). For human single nucleus RNA-seq data, genes in each module were mapped to 1:1 human orthologs (from BioMart), before performing the above analysis.

Analysis of human bulk data

Bulk human RNA-seq data was downloaded from BrainSpan (*9*) (https://www.brainspan.org/static/download.html) and log transformed. For each module, the average expression of the genes of that module were calculated, and the results were plotted.

Differential expression analysis

For each cell type, raw count data was extracted and genes expressed in <5% of cells were removed. We then used limma v3.36.2 (*53*) to perform differential expression analysis, fitting a linear model for each gene with batch and perturbation as covariates. For each perturbation, the associated *P-value* and logFC relative to GFP was calculated, followed by FDR correction.

GO Term Gene Signatures

The mm10 GO ontology was downloaded, and terms with >500 or <5 genes where removed. For each GO Term and each cell type, the genes in that term that appeared in <5% of cells of that cell types were removed. For each term we calculated the average logTPM expression score and fit a linear regression model to this score incorporating

nGene, batch, and perturbation as covariates. *P-values* and effect sizes for each perturbation (relative to GFP) were calculated, and FDR correction was performed.

Analysis of ASD patient data

The UMI count matrix and meta data from Velmeshev et al (*31*) were downloaded from their website (https://autism.cells.ucsc.edu/) and processed with Seurat as above. The subclusters identified in the paper were combined into more general cell types: ODC, Microglia, Vascular, Excitatory, Inhibitory, and Astroglia. For differential expression analysis, we removed data from all individuals of <12 years of age and separated PFC and ACC regions. For each cell type in each region a pseudobulk was constructed and genes expressed in <5% of cells or with <10 reads were removed. DESeq2 v 1.20.0 (*35*) was then used to perform differential expression analysis between the ASD patients and the controls, correcting for sex and age (note: age was encoded as a discrete value, not continuous). We then extracted all genes with 1:1 mouse orthologs (BioMart) and calculated FDR corrected *P-values* on these genes for both ACC and PFC. Only PFC had significant hits.

For each gene and cell type in the final DE table produced (**Table S10**), we calculated the median log fold change (logFC) for that gene's mouse orthologue over all perturbations from the Perturb-Seq data (see **Differential expression analysis**) and took the absolute value to get an absolute logFC score for each gene. Those genes for whom the sign (+1 or -1) of the median logFC agreed with the sign in the human data had their absolute logFC score multiplied by 1; those that disagreed had their absolute logFC score multiplied by -1, such that genes whose direction of change in the Perturb-Seq data agreed with the human data had positive scores, and those whose direction of change disagreed had negative scores. Finally, we binned genes into 5% wide bins based on the % of cells expressing the gene in the Perturb-Seq data, and assigned p-values to each gene based on the percent of genes in the same bin that had an equal or higher score. Finally, the list was filtered to contain only genes also differentially expressed in the human ASD data, and FDR correction was performed.

Scoring of PsychEncode modules in Perturb-Seq single cell data

PsychEncode modules (*34*) were downloaded from the *Science* website, and 1:1 mouse orthologs were extracted for the genes in each module. The same linear regression analysis that was used on our WGCNA modules to determine effect size was applied to the PscyhEncode modules (using all cells instead of just one cell type), as was correlation analysis.

Cell type gene expression

Expression data for the E18.5 mouse brain (9k dataset) was downloaded from the 10X website (*10*). The WT P7 data were generated from this paper. The P7 fastq files were

run through the standard Cellranger pipeline. The data from both datasets were loaded into Seurat separately and transformed to log counts per million. Cells with <500 genes were removed in both datasets. Variable genes were found using FindVariableGenes with x.low.cutoff=1, and the data was scaled with ScaleData, correcting for nUMI. PCA was performed, followed by TSNE and clustering with FindClusters. Cell types were identified with marker genes, and contaminating/vascular cell types were removed.

In each dataset MAST (*54*) was used to find the differentially expressed genes in each cluster, relative to all cells outside that cluster. This was done correcting for the scaled nUMI and removing genes that occurred in less than 10 cells. Average expression was calculated for each gene in each cluster.

Figures S1-S14

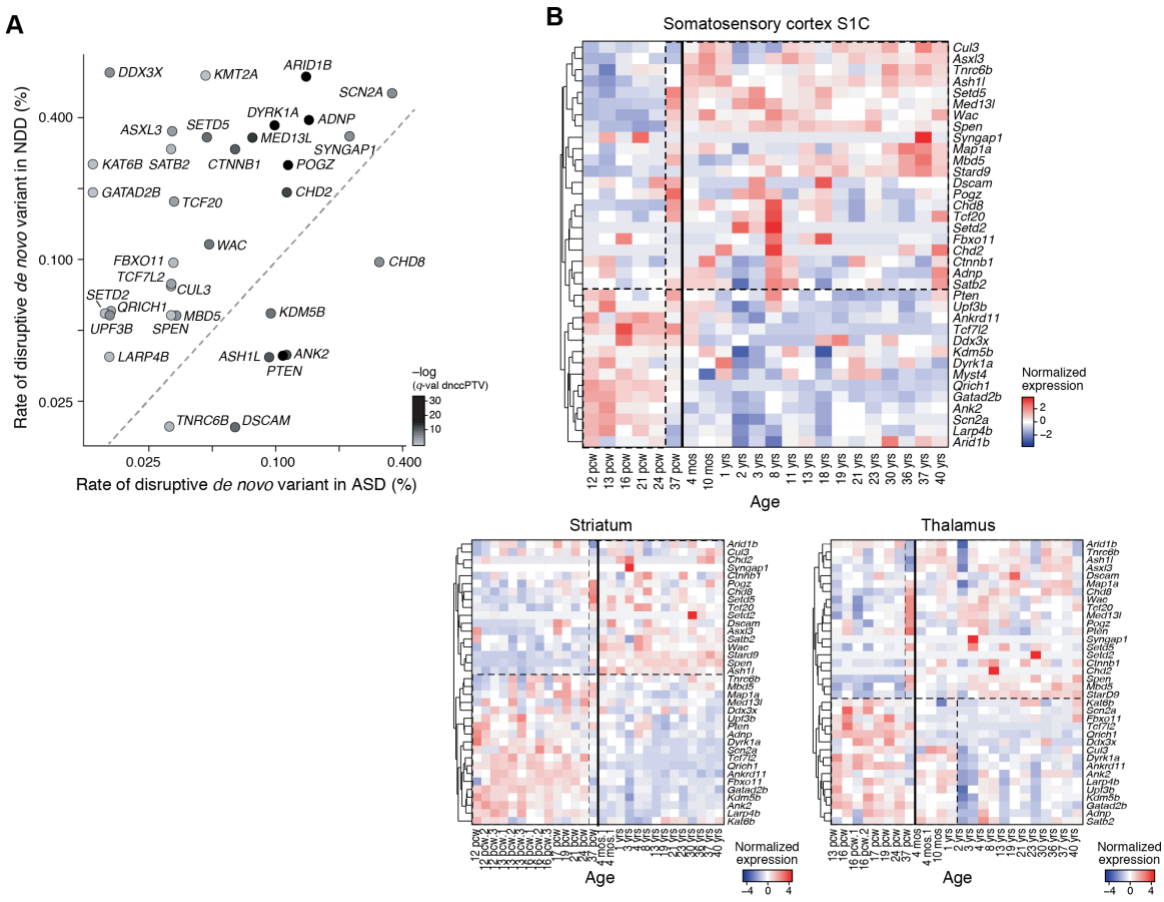

Figure S1. (A) The frequency of *de novo* loss-of-function variants in ascertained Autism Spectrum Disorders (ASD) and neurodevelopmental delay (NDD) cases for the 35 risk-associated genes included the Perturb-Seq analysis. *Q-value* was calculated based on the de novo and case control (dncc) data. This data comes from Satterstrom *et al* (*30*). (B) Gene expression of a panel of selected ASD/ND *de novo* risk genes in human somatosensory cortex (S1C), striatum, and thalamus across the Allen Brain Atlas BrainSpan postmortem samples (*9*). Dendrogram indicates hierarchical clustering by rows.

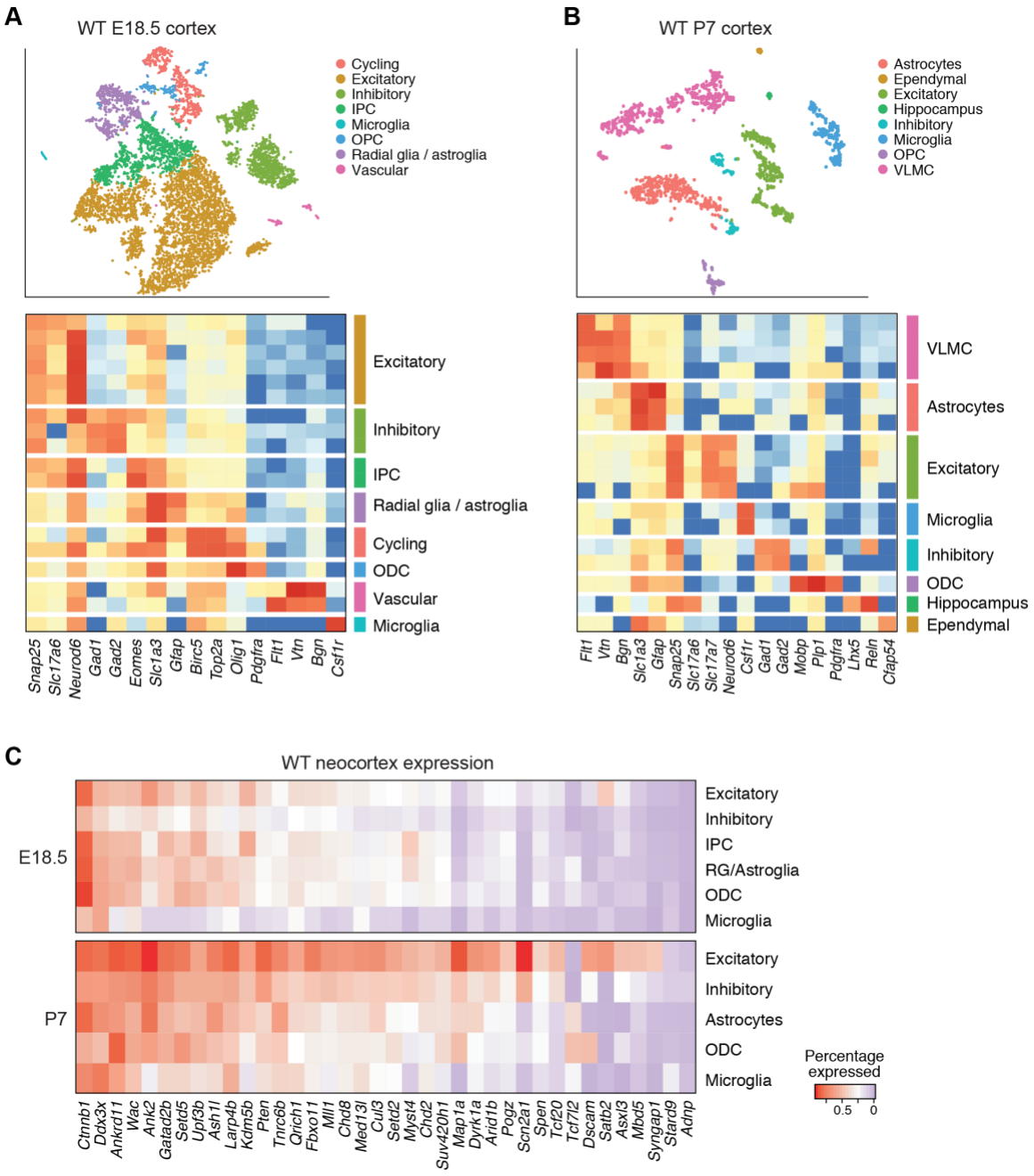

Figure S2. (A-B) Cell type clusters from E18.5 (public data from 10x Genomics) and WT P7 (data generated from this work) neocortex, as well as expression of cell-type marker genes across identified cell clusters. (C) Expression of the 38 initially-selected risk-associated genes in the cell clusters from E18.5 and P7 wild-type cortex.

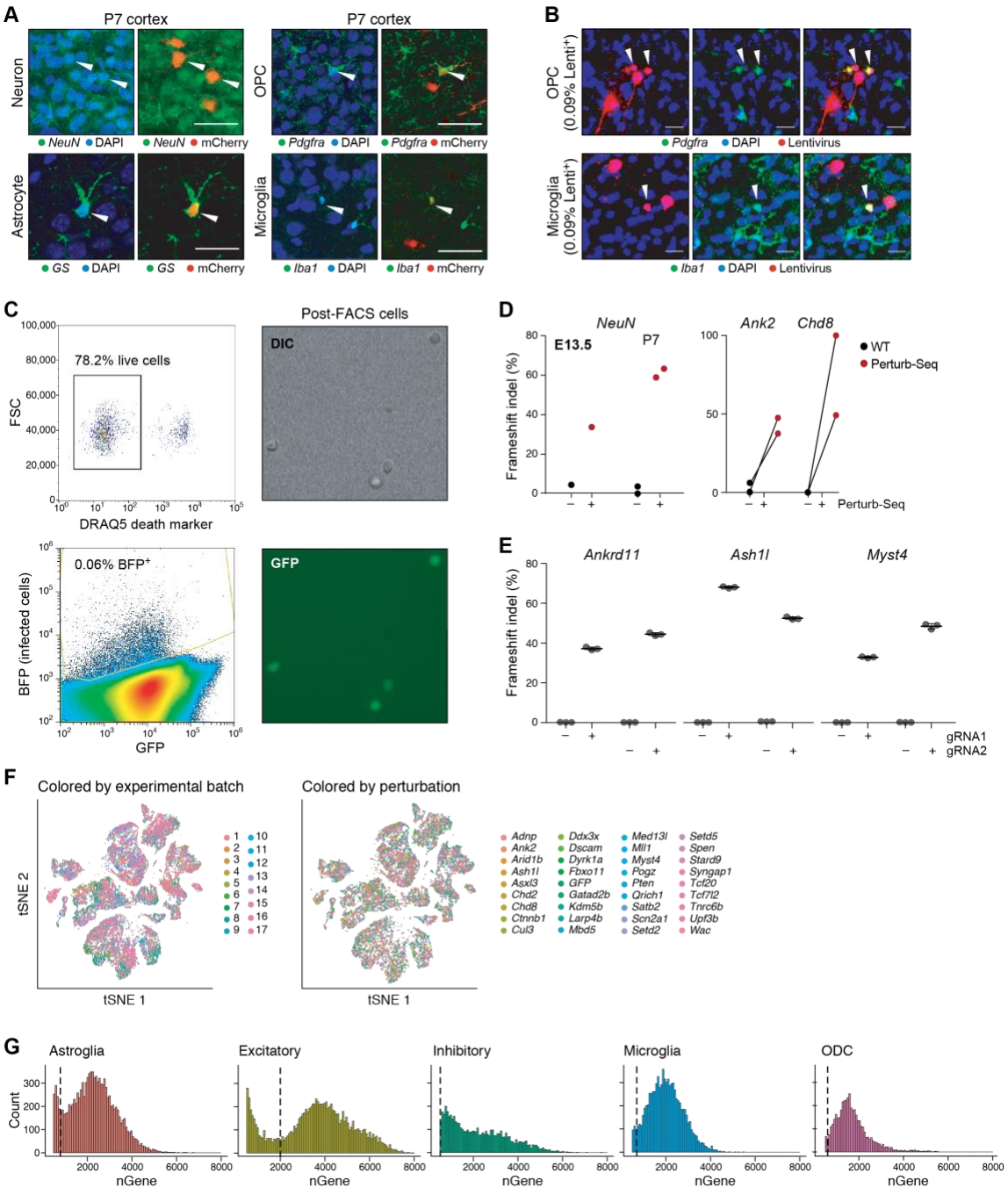

Figure S3. (A-B) Lentiviral injection at E12.5 sparsely infects neurons (NeuN$^+$), astrocytes (Glutamine Synthase [GS]$^+$), oligodendrocyte precursor cells (PDGFRA$^+$), and microglia and macrophages (IBA1$^+$) in the P7 neocortex (indicated by white arrows). Scale bar is 50μm. *In vivo* Perturb-Seq lentiviral vector with an mCherry expression cassette allows immunohistochemical identification of the targeted cell types. Lentiviral vector expression, indicated by BFP expression as well as perturbation barcode expression, was present in microglia (and likewise in all cell types included in this study, fig S4E-F). (C) The proportion of live cells after FACS purification is 78.2%, and <0.1% of total dissociated cortical cells are BFP$^+$ (indicated by polygons). (D-E) Frameshift

insertion/deletion rates of the targeted loci by CRISPR/Cas9 genome editing (D) in the infected cells *in vivo*, and (E) in mouse embryonic stem cells *in vitro* as a control, for each gRNA. (F) Distribution of the perturbed cells in the 5 major cell types, across 17 different libraries (independent experimental batches) (left) and 35 different perturbation groups (right). (G) Number of genes detected in each cell type in the Perturb-Seq single-cell RNA-seq data. Quality control cutoffs for each cell type are marked by black vertical bars.

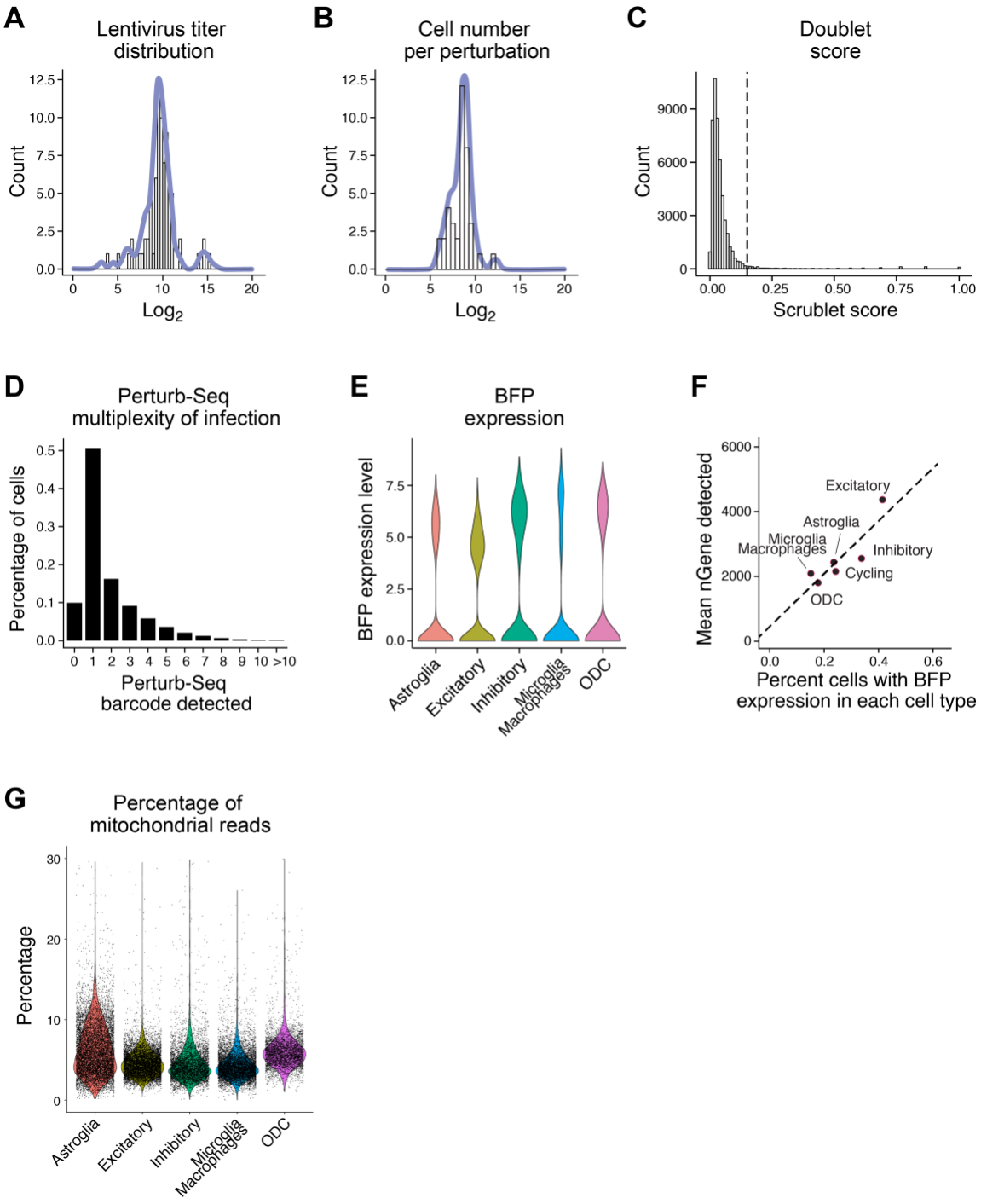

Figure S4. (A) The distribution of each perturbation vector in the lentiviral pool. (B) The distribution of cell numbers from each ASD/ND perturbation group. (C) Estimated doublet score in the Perturb-Seq data using the Scrublet package; the black vertical bar represents the cutoff above which a "cell" is declared as a doublet. (D) The distribution of the number of perturbation barcodes detected per cell. (E) BFP is one of the genes with the highest expression level, detected in all 5 cell types. (F) BFP expression level is

correlated with the number of genes detected in each cell type. (G) Percentage of UMI from reads mapping to the mitochondrial genome in each cell type.

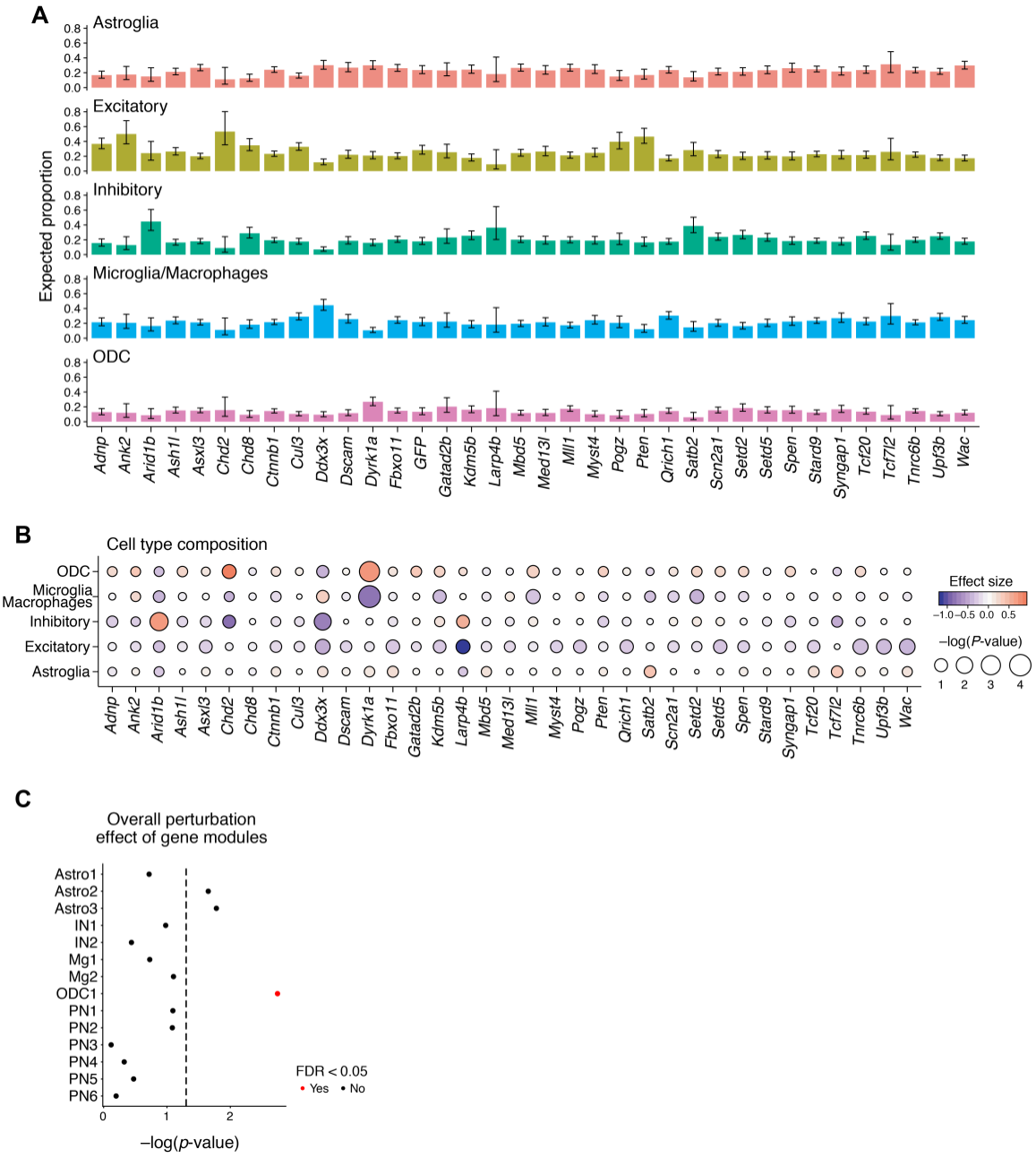

Figure S5. (A) Proportion of the 5 major cell types in each perturbation group. (B) Poisson regression for differences of cell type composition compared to the GFP control group. The size of the dots corresponds to base 10 log (*P-value)*, the color to effect size. (C) Nonparametric ANOVA analysis shows that perturbation status overall (as opposed to the status of individual target genes) explains a significant portion of the variation in one glial module, ODC1.

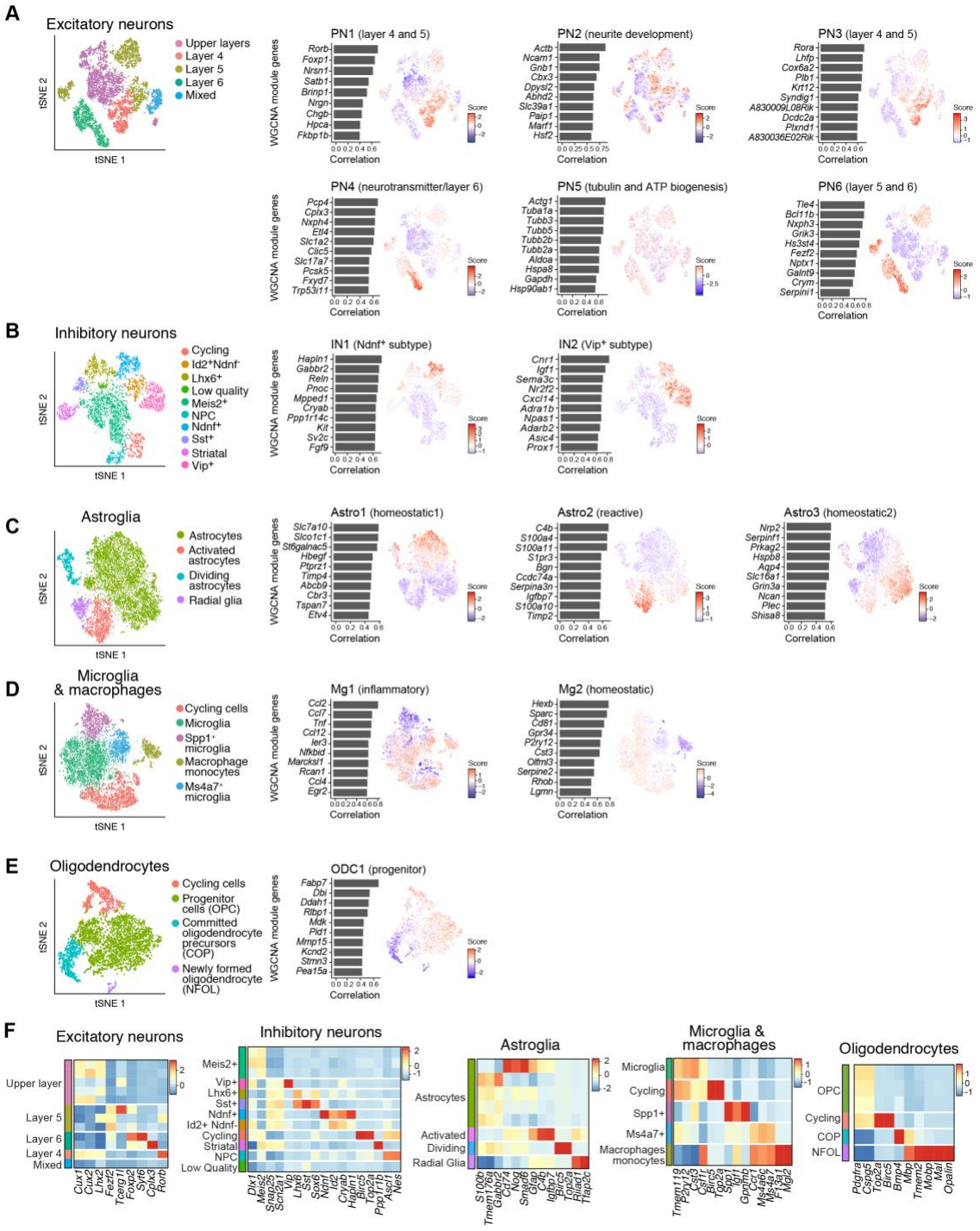

Figure S6. (A-E) Subclusters of each major cell class and feature plots of scores of gene modules identified by WGCNA, labelled by associated cell subtypes or biological processes. (F) Expression of key cell type marker genes in each subtype.

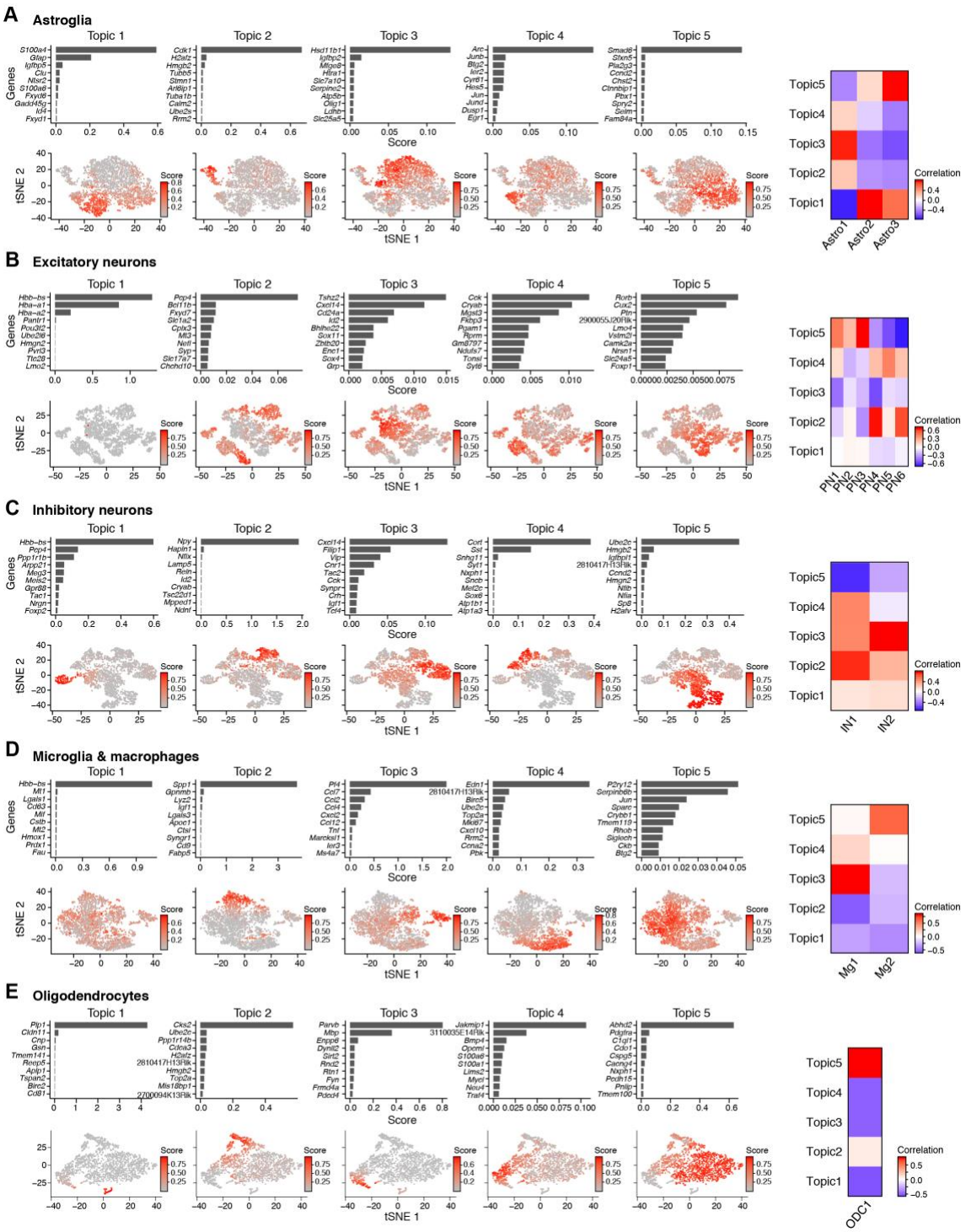

Figure S7. Topics identified by structural topic modeling (STM) and their correlation with WGCNA modules. Gene score indicates the lift score from STM analysis; a gene with high gene score is highly representative of the given topic.

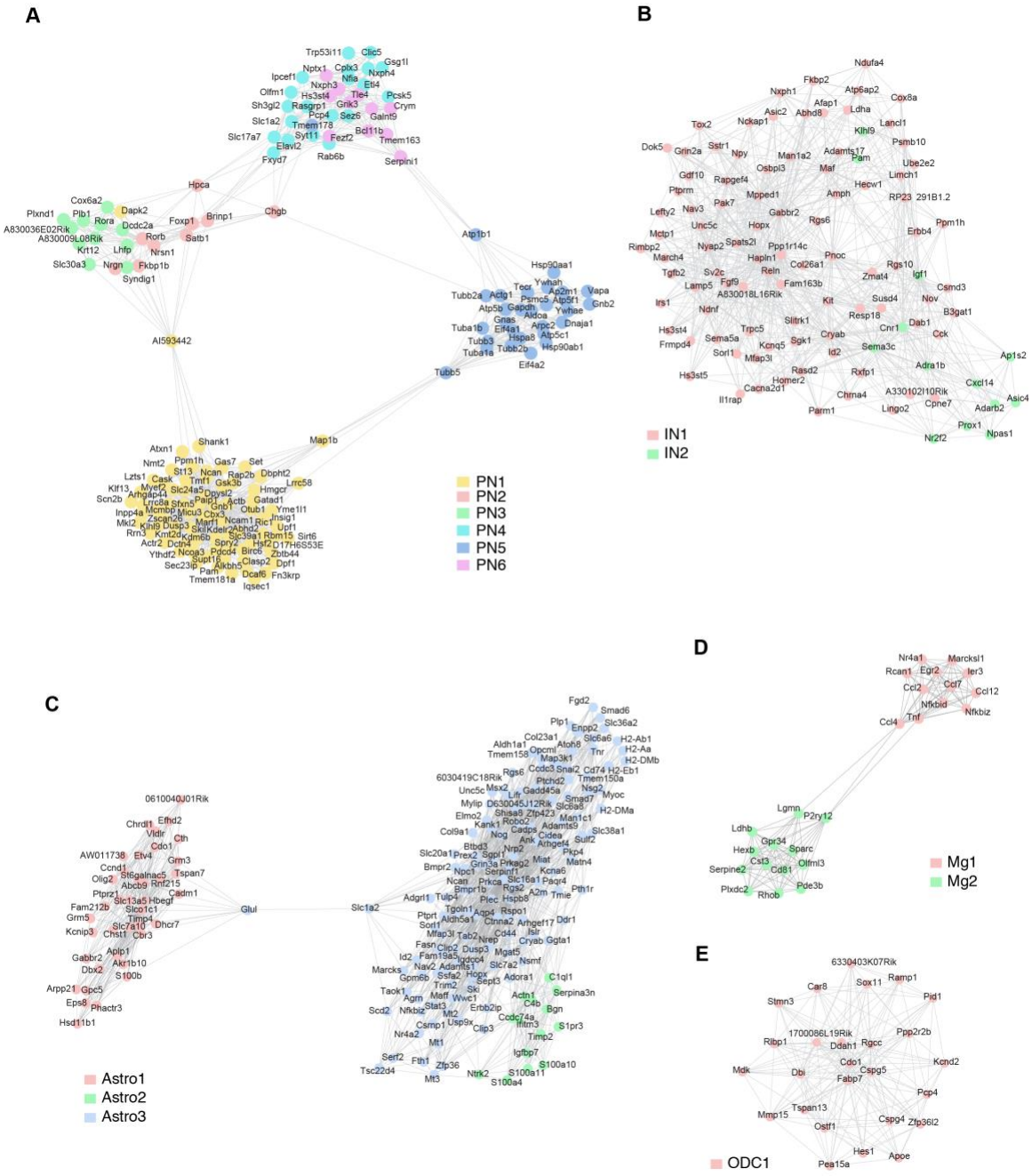

Figure S8. Graph visualization of the 14 WGCNA network modules in 5 major cell types. Pairwise correlation was computed between each two genes, and a directed 11 nearest neighbor graph was generated and plotted with igraph.

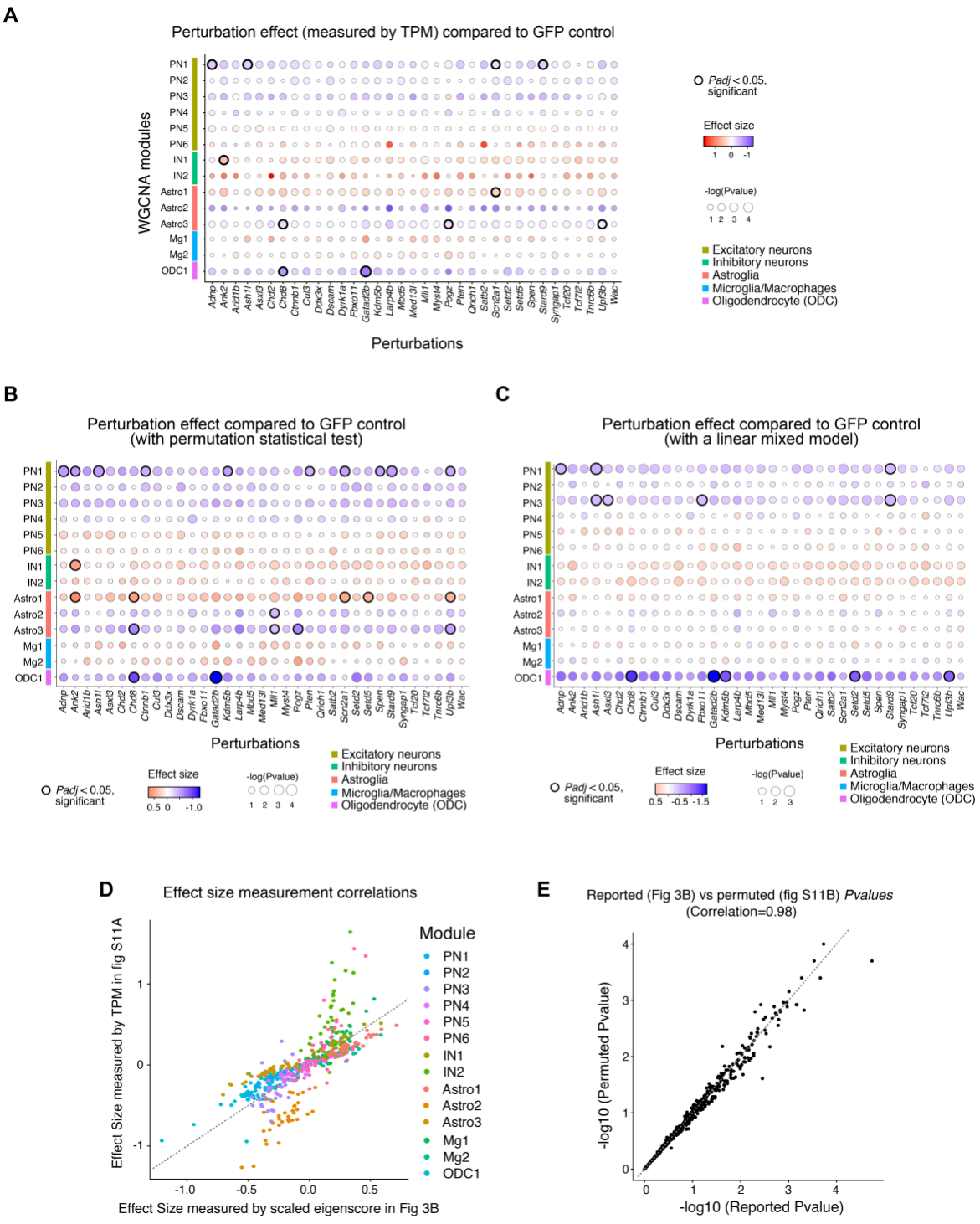
A
Perturbation effect (measured by TPM) compared to GFP control
WGCNA modules
PN1
PN2
PN3
PN4
PN5
PN6
IN1
IN2
Astro1
Astro2
Astro3
Mg1
Mg2
ODC1
Perturbations
Padj < 0.05, significant
Effect size
-log(Pvalue)
Excitatory neurons
Inhibitory neurons
Astroglia
Microglia/Macrophages
Oligodendrocyte (ODC)
B
Perturbation effect compared to GFP control (with permutation statistical test)
C
Perturbation effect compared to GFP control (with a linear mixed model)
D
Effect size measurement correlations
Effect Size measured by TPM in fig S11A
Effect Size measured by scaled eigenscore in Fig 3B
Module
E
Reported (Fig 3B) vs permuted (fig S11B) Pvalues
(Correlation=0.98)
-log10 (Permuted Pvalue)
-log10 (Reported Pvalue)

Figure S9. (A) ASD/ND risk gene perturbation effects in different WGCNA gene modules compared to GFP controls, measured by TPM. Dot color corresponds to effect size, dot size corresponds to base 10 log(*P-value*). *P-values* were extracted from the analysis in Fig 3; *Padj* was calculated using Benjamini & Hochberg FDR correction. (B-C) ASD/ND risk gene perturbation effects in different WGCNA gene modules compared to GFP controls, measured as Fig. 2B, with an alternative method for calculating *P-values*: instead of using the naive *P-value* output by the linear model (as Fig. 2B), they were calculated using a permutation test (B) or through a linear mixed model (C). *Padj* was calculated using Benjamini & Hochberg FDR correction. Dot color corresponds to effect size, dot size corresponds to base 10 log(*P-value*). (D) Correlation of the Perturb-Seq effect size measured by TPM (in fig. S9A) and those measured by scaled eigen score (in Fig. 2B). (E) Correlation of the reported *P-values* generated by a linear model (in Fig. 2B) and those measured by a permutation test (in fig. S9B).

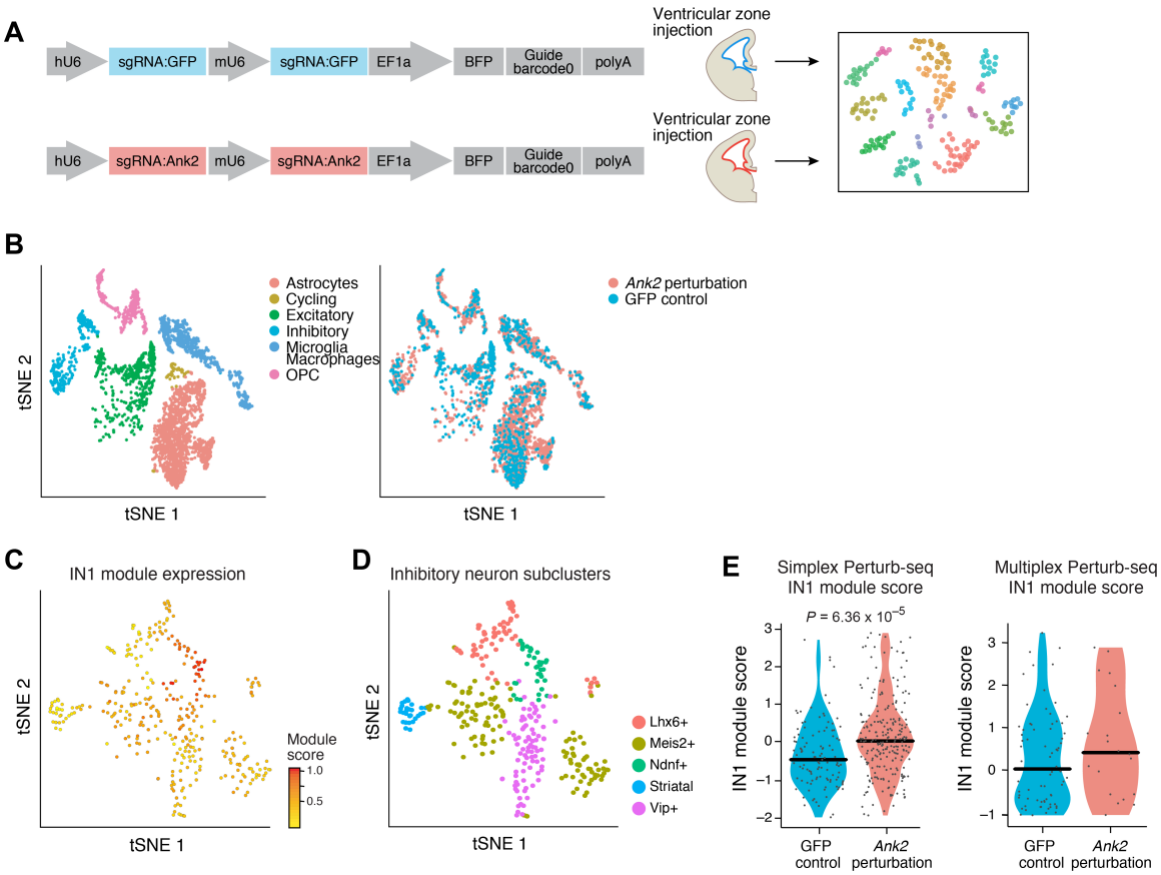

Figure S10. (A) Schematics of simplex Perturb-Seq of the ASD/ND risk gene *Ank2* and a GFP control. (B) Cell type clusters from P7 neocortical simplex *Ank2* Perturb-Seq. (C-D) Subtype clusters of inhibitory neurons from the simplex *Ank2* Perturb-Seq. (E) Simplex dataset expression of the gene module IN1 identified in the pooled Perturb-Seq analysis.

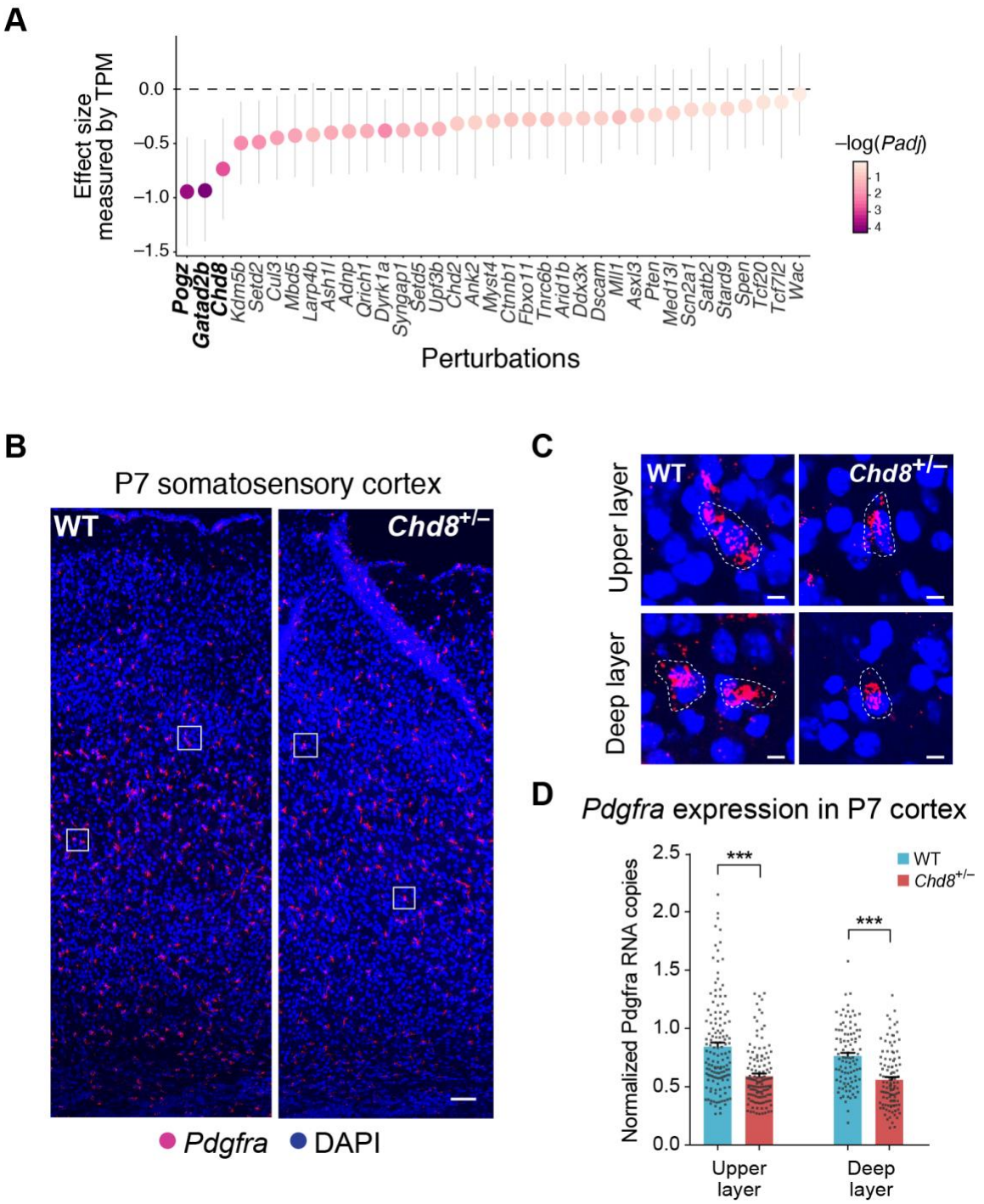

Figure S11. (A) ASD/ND risk gene perturbation effects in gene module ODC1 compared to GFP controls, measured by change in log TPM. (B-C) *In situ* hybridization for *Pdgfra*, a marker of oligodendrocyte precursor cells, in the somatosensory cortex of P7 *Chd8*$^{+/-}$ animals and wild-type littermates. Dotted lines in C indicate individual *Pdgfra*-positive nuclei at higher magnification (white boxes in panel B). Scale bar is 100μm (panel B) and 10μm (panel C), respectively. (D) Quantification of *Pdgfra* expression in

somatosensory cortex of *Chd8*$^{+/-}$ and wild-type littermates. Each dot represents the gene expression measurement from one cell; error bars represent standard error of the mean. n=3 animals per genotype.

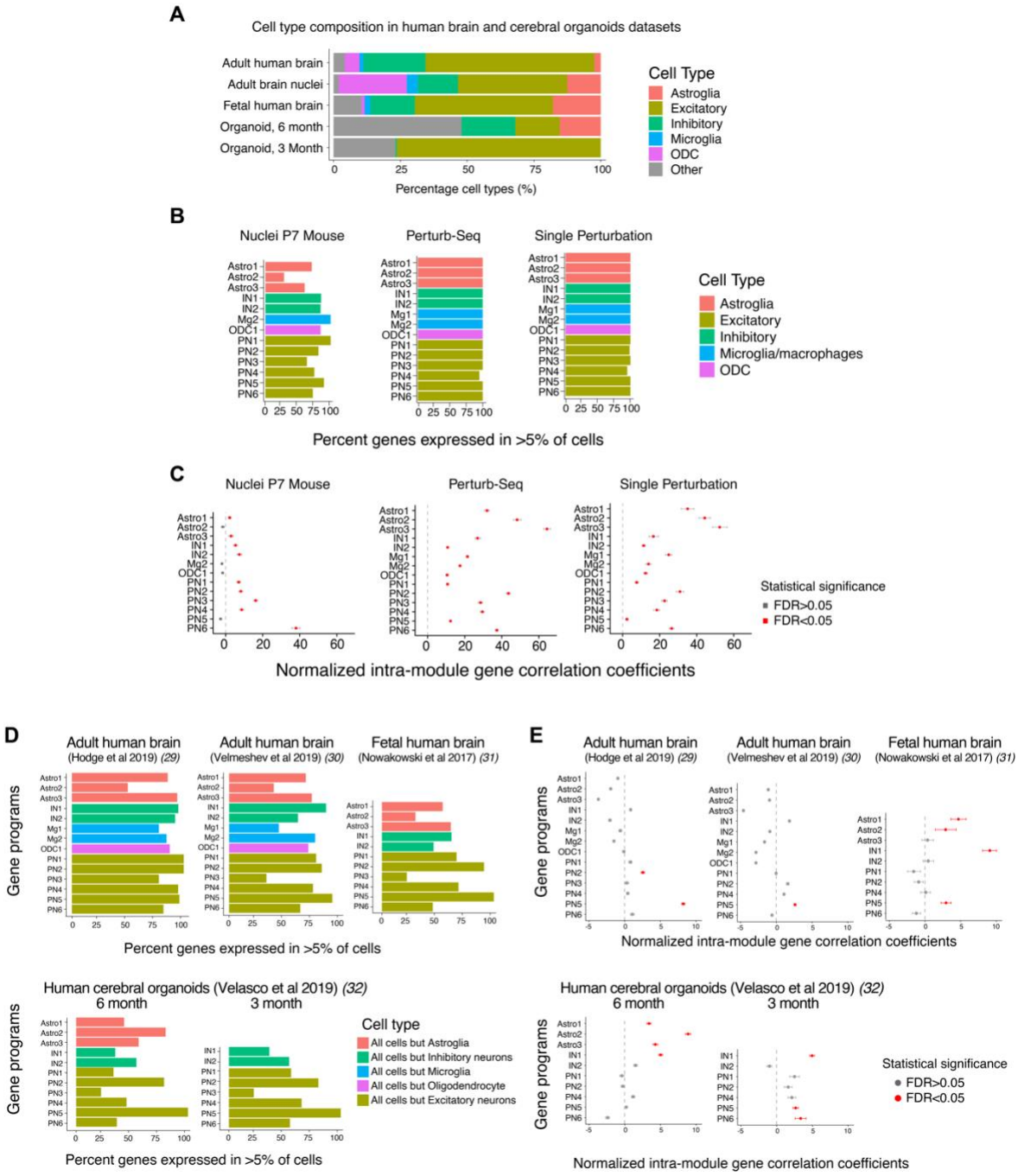

Figure S12. (A) Cell type composition in each human brain and human brain organoid dataset. (B-C) Metrics used for human conservation analysis, repeated on mouse cells as a control (compare Fig. 4A-B). (B) Percent of genes in each gene module expressed in at least 5% of cells in the P7 mouse brain nuclei, Perturb-Seq dataset (whole cell), and simplex Perturb-Seq (whole cell) scRNA-seq datasets. (C) Normalized average pairwise correlation of gene expression within each gene module in each mouse dataset. Bars represent 95% confidence intervals. (D-E) Gene expression and modularity analyses

analogous to Figure 4A-B, performed on the non-associated cell types of each module as a control, shows a lower proportion of comparisons with significant correlation coefficients and a much lower strength of correlations than in the associated cell types (Figure 4A-B).

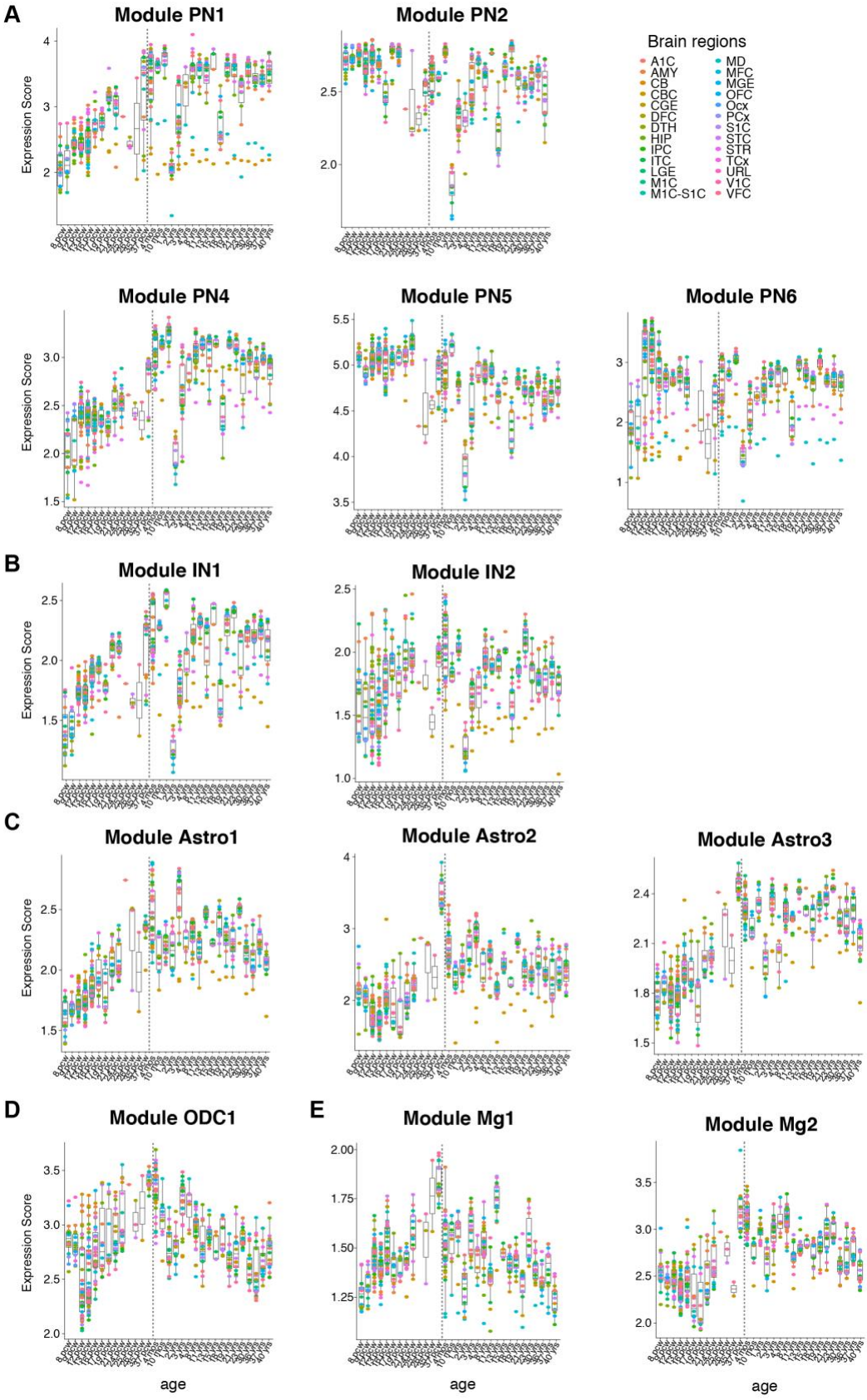
A
Module PN1
Module PN2
Brain regions
A1C
AMY
CB
CBC
CGE
DFC
DTH
HIP
IPC
ITC
LGE
M1C
M1C-S1C
MD
MFC
MGE
OFC
Ocx
PCx
S1C
STC
STR
TCx
URL
V1C
VFC
Module PN4
Module PN5
Module PN6
B
Module IN1
Module IN2
C
Module Astro1
Module Astro2
Module Astro3
D
Module ODC1
E
Module Mg1
Module Mg2
Expression Score
age

Figure S13. Module expression over developmental time in human brain tissues across regions (BrainSpan data (*9*)) in 5 major cell types.

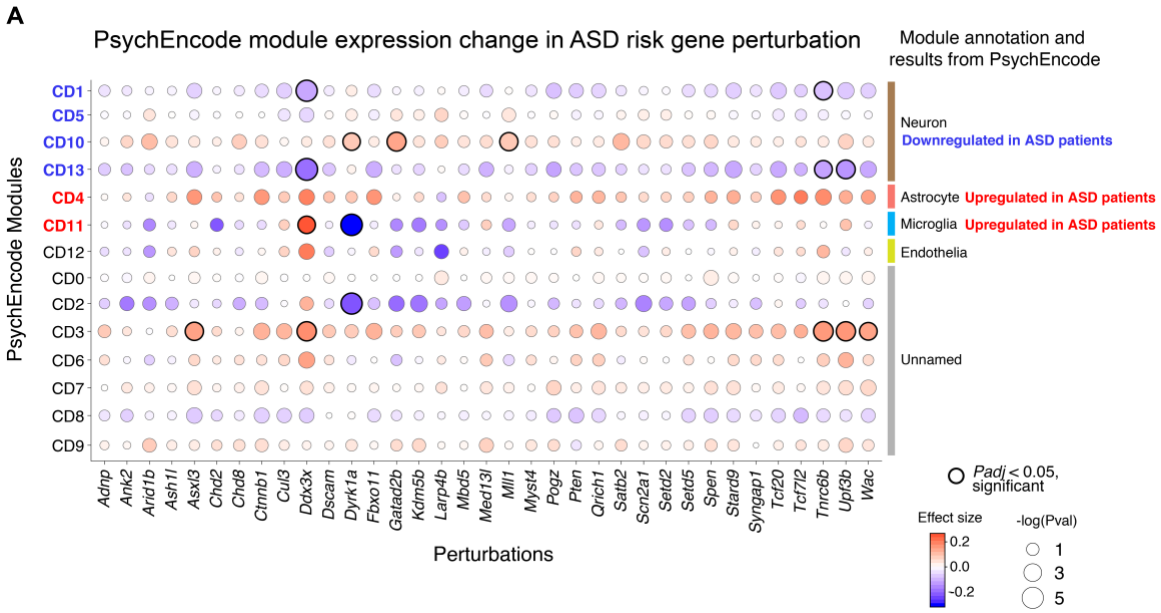

Figure S14. (A) ASD/ND risk gene perturbation effects in our Perturb-Seq data (compared to GFP control) on 14 gene modules from the PsychEncode study comparing ASD patient and control brain tissue (*34*). Dot color corresponds to effect size, dot size corresponds to base 10 log(*P-value*). *Padj* was calculated using Benjamini & Hochberg FDR correction.

Tables are presented as individual Excel files.

Table S1. ASD/ND risk gene list and their effect in the patient cohort.
Table S2. WGCNA gene module gene lists.
Table S3. Structural topic modeling fitted model.
Table S4. Effect size estimate of each ASD/ND risk gene perturbation and nonparametric ANOVA analysis in the cortex in WGCNA modules and STM topics.
Table S5. gRNA design for the ASD/ND risk gene perturbations.
Table S6. Parameters used in Seurat for cell type clustering.
Table S7. Analysis of differential gene expression from Perturb-Seq data.
Table S8. Analysis of ASD/ND risk gene perturbation effect for GO term gene signatures.
Table S9. Alternative effect size and statistical measurements of Perturb-Seq.
Table S10. Analysis of human ASD patient data (Velmeshev et al (*31*)) and comparison with Perturb-Seq.